tion on the normal to the (101) plane (**k**), and the macroscopic contribution greatly enhances the $\perp b$ lattice sum. The second-order splittings calculated for the five vibronic bands are 214, 399, 342, 168, and 125 cm^{-1} with the $\perp b$ bands at higher energy.[41] In the absence of the macroscopic term, the *b*-axis states would be calculated to be at higher energy. The splittings predict that the spectrum $\perp b$ should be shifted to higher energy and that there should be some merging of bands in the high-energy region. It is evident that the calculations are not in good quantitative agreement with experiment since the experimental splittings are not as large as predicted. Indeed, there is no observed splitting of the O–O band although the higher vibrational bands $\perp b$ are clearly at higher energy. Clark and Philpott have observed the dependence of Davydov splittings on the orientation of the wave vector for spectra measured on several faces of the anthracene crystal.[42] They have noted that calculations of dipole sums in which the macroscopic component is substantial tend to overestimate the band splittings. It is possible that a similar situation obtains in our spectra of the 2700-Å pyrazine system.

We have also carried out calculations on the tetramethylpyrazine spectra. Three electronic transitions with hexane solution energies and intensities listed in Table II were included in our treatment. Again the second-order calculation does not indicate any significant change in oriented gas intensities. In this case although the dipole strengths of the interacting levels are larger, the dipole interactions between inequivalent molecules in the lattice are small, and there is cancellation of contributions from different inequivalent molecules. It should be noted that the apparent enhancement of the *b*-axis $^1B_{3u} \leftarrow {}^1A_{1g}$ absorption observed in the crystal spectrum is not predicted by the calculations. The calculations indicate very small mixing of the $^1B_{3u}$ *b*-axis factor group state with the overlapping $^1B_{2u}$ state and even smaller mixing of *a*-axis factor group states.

Acknowledgments. We gratefully acknowledge the receipt of grants from the City University Faculty Research Program in support of this work. We thank Dr. William A. Eaton for many helpful and stimulating discussions.

---

[41] The first-order splittings are 217, 410, 351, 170, and 126 cm^{-1} and are, therefore, not greatly changed in the second-order treatment.

[42] L. B. Clark and M. R. Philpott, *J. Chem. Phys.*, **53**, 3790 (1970).

Crystal Nucleation Studies in Supercooled Mesomorphic Phases of Cholesteryl Derivatives[1]

John M. Pochan* and Harry W. Gibson

Contribution from the Xerox Corporation,
Rochester Corporate Research Center, Webster, New York 14580.
Received October 8, 1971

Abstract: Classical nucleation rate theory derived for isotropic systems has been applied for the first time to crystallization from the liquid-crystalline phases of cholesteryl esters and binary mixtures thereof. Interfacial energy parameters are an order of magnitude less in these systems than in normal isotropic systems and are shown to be a function of ester chain length, the type of mesophase, and composition in binary mixtures. Phase diagrams are also determined for binary mixtures.

The study of rate of nucleation or growth of crystals from supercooled liquids has, in the past, yielded important thermodynamic parameters. Studies have been conducted on monomeric and polymeric systems exhibiting liquid and crystal phases.[2,3] The degree of supercooling in pure and mixed mesomorphic systems is unique. Supercooling by as much as 86° for a pure compound has been achieved in this study with the resultant liquid crystal stable to recrystallization for several minutes.

In this paper, we report a unique application of nucleation theory to crystallization from supercooled smectic and cholesteric liquid-crystalline states. In association with this nucleation rate study, phase diagrams of mixed cholesteric systems have been obtained in order to study the effect of one mesomorphic compound or state on another.

Theory

Using transition-state theory, Turnbull and Fisher developed an expression for the rate of homogeneous nucleation in condensed systems.[4] The steady-state nucleation rate per unit volume is given by

$$\mathrm{d}n/\mathrm{d}t = N_0 \exp(-E_\mathrm{d}/RT)\exp(-\Delta F^{\ddagger}/RT) \quad (1)$$

where E_d is the free energy of activation for transport across a liquid–nucleus boundary; $\Delta F^{\ddagger}$ is the free energy change associated with nucleus formation, and $N_0 = M_0kT/h$, where M_0 is the number of molecules per unit volume in the liquid, *h* equals Planck's constant, and *k* is Boltzmann's constant.

Equation 1 describes nucleation in terms of two different rate processes. At temperatures below the nuclea-

---

[1] A portion of this work has been previously reported: J. M Pochan and H. W. Gibson, *J. Amer. Chem. Soc.*, **93**, 1279 (1971).

[2] L. Mandelkern, N. J. Jain, and H. Kim, *J. Polym. Sci.*, **6**, 165 (1968).

[3] D. G. Thomas and L. A. K. Stavely, *J. Chem. Soc.*, 4569 (1952).

[4] D. Turnbull and J. C. Fisher, *J. Chem. Phys.*, **17**, 71 (1949).

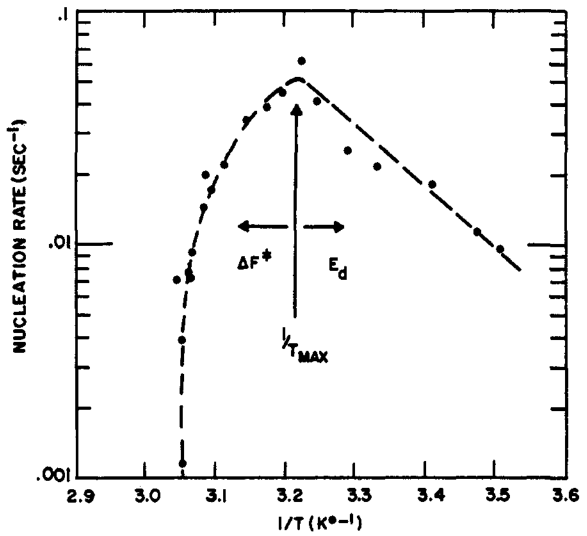

Figure 1. Ln (nucleation rate) *vs.* $1/T$ for cholesteryl nonanoate.

tion rate maximum the process is diffusion or viscosity controlled. In this region, the molecules at the liquid crystal–crystal interface have enough energy to be activated (to cross an energy barrier to the face of the crystal); however, the microscopic viscosity of the medium retards this molecular realignment. At temperatures above the rate maximum, the microscopic viscosity of the medium is low enough so as not to be rate limiting and the thermal barrier then becomes rate limiting. This phenomena is exemplified in Figure 1 where a plot of ln (nucleation rate) *vs.* $1/T$ for cholesteryl nonanoate is shown.

Many derivations of the dependence of critical size and critical free energy on nuclear shape have been given previously.[5,6] The cylindrical nuclear model was chosen. Contributions of strain and edge free energies have been neglected.[2] Equation 1 then becomes

$$\mathrm{d}n/\mathrm{d}t = N_0 \exp(-E_\mathrm{d}/RT) \exp\{[8\pi\sigma_\mathrm{u}^2\sigma_\mathrm{e}/\Delta H^2RT] \times [T_\mathrm{m}^2/(\Delta T)^2]\} \quad (2)$$

$$= N_0 \exp(-E_\mathrm{d}/RT) \exp\{-KT_\mathrm{m}^2/T(\Delta T)^2\} \quad (3)$$

where ΔH is the enthalpy of fusion, σ_u and σ_e are the lateral and end-to-end molecular interfacial surface energies, and $\Delta T = T_\mathrm{m} - T$. Adding the more general preexponential temperature term the final form of the nucleation rate equation used in this study is then

$$\ln \text{rate} = \ln C + \ln T - E_\mathrm{d}/RT - KT_\mathrm{m}^2/T(\Delta T)^2 \quad (4)$$

It should be noted that there is a distinct possibility that heterogeneous nucleation occurs because of the large samples used. In this case, the theory used to interpret the experimental nucleation data changes slightly. $\Delta F^{\ddagger}_{\text{homogeneous}}$ is now replaced by $f(\theta)\Delta F^{\ddagger}_{\text{homogeneous}}$ and $f(\theta)$ varies between 0 and 1. However, since there is no way of accurately determining $f(\theta)$ in this experiment, the results are presented using eq 4.

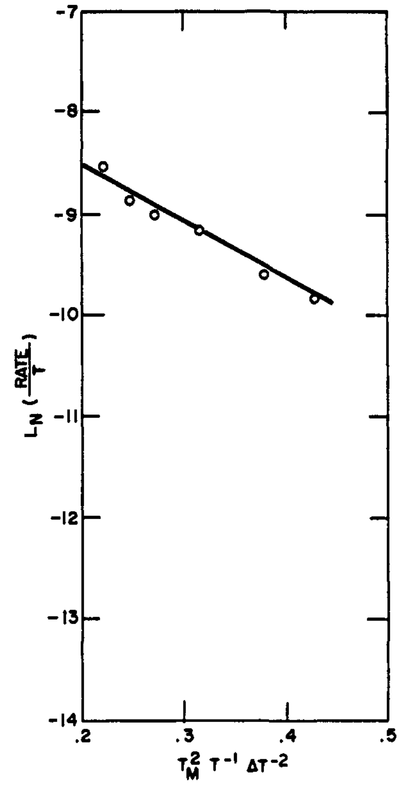

Figure 2. Ln (rate/T) *vs.* $T_\mathrm{m}^2/T(\Delta T)^2$ for cholesteryl nonanoate for temperatures above 310°K.

Experimental Section

Materials. Cholesteryl formate, propionate, hexanoate, and nonanoate were purchased from Eastman, Cholesteryl pentanoate was synthesized in 98% yield from cholesterol and pentanoyl chloride. All the esters were purified by repeated recrystallization from ethanol or ethanol–ethyl acetate. Purity was checked by thin layer chromatography and elemental analysis.

Nucleation Rate Measurements. Mixtures were prepared by removing the solvent ($CHCl_3$) from a filtered solution of the weighed components in a 15 × 1 (i.d.) cm glass tube. The tube was degassed and sealed at 10^{-5} mm. The bath consisted of either a 3-l. beaker filled with water and equipped with a Bronwill Thermomix Junior thermostat or a Lauda 10-l. thermostated water bath. In both cases, a calibrated Lauda thermometer graduated in 0.5° increments was employed for temperature readout. Temperature control was ±0.1°.

The sample tube was gently heated in a flame until the sample was completely isotropic, care being taken not to overheat. The sample was spread in a thin film by rotating the tube, which was then plunged into the thermostated bath. Time measurement was begun at this point using a Precision Scientific timer. When the first small crystal was visually observed (in some cases with the aid of a 2X magnifying glass), the time to 0.1 sec was recorded. Seven to twelve repeat readings were taken. Nucleation times were corrected for heat transfer from the sample tube to the bath.[7]

Differential Scanning Calorimetry. Mixtures were made by melting the weighed ingredients, mixing thoroughly, cooling to ~0° to prevent separation, and then allowing them to crystallize at room temperature. Samples were weighed to ±0.01 mg on a Cahn electrobalance. A calibrated Perkin-Elmer DSC-1B was employed to measure heats of transition at a scanning rate of 10°/min. Estimation of crystal to mesomorphic transition temperatures is good to ±2° for the mixtures and ±1.0° for pure compounds. The mesomorphic to isotropic liquid transition temperatures are believed to be accurate to ±1° for both mixtures and pure compounds. The enthalpies for the transitions were determined by comparison of the areas under the peaks to that under the peak for indium and benzoic acid standards.

---

(5) (a) L. Mandelkern, "Crystallization of Polymers," McGraw-Hill, New York, N. Y., 1964; (b) L. Mandelkern, J. G. Faton, and C. Howard, *J. Phys. Chem.*, **69**, 956 (1965).

(6) L. Mandelkern, J. G. Faton, and C. Howard, *ibid.*, **68**, 3386 (1964).

(7) R. Bird, W. Stewart, and E. Lightfoot, "Transport Phenomena," Wiley, New York, N. Y., 1960, p 356.

Table I. Results for Pure Cholesteryl Derivatives

Derivative	ΔH,[a] cal/g	T_m, °C	ΔS,[a] eu	T at max rate, °C	K,[a] °K	ρ, g/ml	$\bar{\sigma}$,[a] ergs/cm^2
Formate	12.5 (±0.5)[b]	96[b]	14.1 (±1.1)	~40	16.1 (±2.4)	0.96	2.82 (±0.23)
Propionate	12.8 (±0.5)[b]	97[b]	15.3 (±1.2)	~60	0.869 (±0.154)	0.95	1.07 (±0.10)
Pentanoate	9.52 (±0.21)	93	12.4 (±1.0)	~60	2.01 (±0.10)	0.95	1.17 (±0.08)
Hexanoate	13.3 (±0.2)	97	17.4 (±1.0)	~50	2.56 (±0.79)	0.94	1.57 (±0.17)
Nonanoate	10.6 (±0.4)	80	15.8 (±1.3)	~40	11.0 (±1.4)	0.98	2.25 (±0.16)
Chloride	13.0 (±0.2)	96	14.3 (±0.9)	~40	38.5 (±3.6)	0.98	3.92 (±0.16)

[a] Standard deviations given in parentheses. [b] Taken from ref 10.

Table II. Results for Mixtures of Cholesteryl Nonanoate and Cholesteryl Hexanoate

Mol % hexanoate	ΔH,[a] cal/g	T_m, °C	ΔS,[a] eu	T at max rate, °C	K,[a] °K	ρ, g/ml	$\bar{\sigma}$,[a] ergs/cm^2
0	10.6 (±0.4)	80	15.8 (±0.7)	~40	11.0 (±1.4)	0.98	2.25 (±0.16)
10.7	8.28 (±0.21)	72	12.6 (±0.5)	~15	19.7 (±3.6)	0.98	2.31 (±0.19)
26.6	6.53 (±0.65)	67	9.97 (±1.10)	~20	7.81 (±2.34)	0.97	1.45 (±0.25)
52.1	8.65 (±0.34)	60	13.1 (±0.6)	~35	0.347 (±0.023)	0.96	0.624 (±0.031)
76.5	7.03 (±0.30)	68	10.2 (±0.5)	~40	0.767 (±0.059)	0.95	0.697 (±0.042)
90.7	9.20 (±0.40)	92	12.4 (±0.6)	~40	6.06 (±0.42)	0.94	1.64 (±0.08)
100	13.3 (±0.2)	97	17.5 (±1.0)	~50	2.56 (±0.79)	0.94	1.57 (±0.17)

[a] Standard deviations given in parentheses.

Data Analysis

Near the maximum rate both terms of eq 3 contribute significantly. Therefore, an evaluation of either of the terms must be done using data as far as possible from this maximum to ensure minimal contribution from the other term. At temperatures above that at maximum rate (T_{max}) a linear least-squares fit of eq 5 using data for which the rate was less than 50% of that at T_{max} was employed to determine K. In Figure 2, a graph of ln (rate/T) *vs.* $T_m^2/T(\Delta T)^2$ for cholesteryl nonanoate at temperatures above the rate maximum does exhibit the linearity predicted by the theory. $\bar{\sigma}$ was calculated from eq 6. In the cases of cholesteryl nonanoate and cholesteryl chloride E_d was evaluated at temperatures below T_{max} in similar fashion using eq 7.

$$\ln (\text{rate}/T) = -KT_m^2/T(\Delta T)^2 + \ln C \qquad (5)$$

$$\bar{\sigma} = \sqrt[3]{RK\rho^2(\Delta H)^2/8\pi} \text{ where } \rho = \text{density (g/cc)} \qquad (6)$$

$$\ln (\text{rate}/T) = -E_d/RT + \ln C \qquad (7)$$

Attempts were made to fit the data over the entire temperature range for cholesteryl nonanoate by varying both K and E_d (eq 4). It was not possible to obtain a good fit over a wide range of these two variables, although the shape could be well approximated. Results reported here for cholesteryl hexanoate and nonanoate and binary mixtures thereof are refinements of our preliminary results.[1]

Results

The results of DSC measurements are listed in Table I. Crystalline melting points of the samples are less accurate than usual DSC determinations because of the broad transition peaks. Microscopic examination reveals this peak broadness is due to partial phase separation of the mixtures upon recrystallization. In some cases, two melting peaks were observed (one usually much larger) and the ΔH listed in Table I is the total of both; the melting temperature is that associated with the larger enthalpy transition. In the cases where two such peaks were observed, both were much lower than either pure component melting points, indicating, as in the microscopic observations, mixed crystalline states. No evidence was found for eutectic mixtures. The phase diagram of cholesteryl nonanoate–cholesteryl hexanoate is given in Figure 3. The crystal melting temperature of the mixtures is linear with composition at low percentages of either component. In a separate study, which will be reported shortly, 13 binary-phase diagrams involving cholesteryl nonanoate have been constructed. At high nonanoate concentrations, the initial slopes are not identical from system to system. Thus, these linear regions do

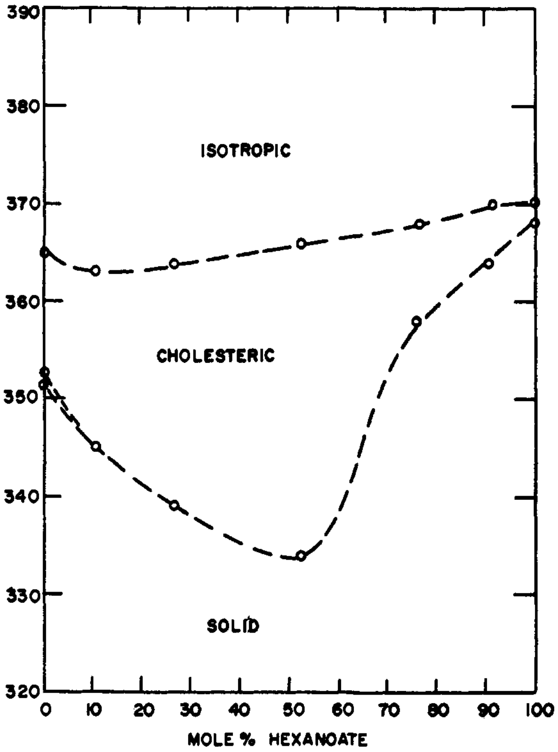

Figure 3. Phase diagram for cholesteryl nonanoate–cholesteryl hexanoate.

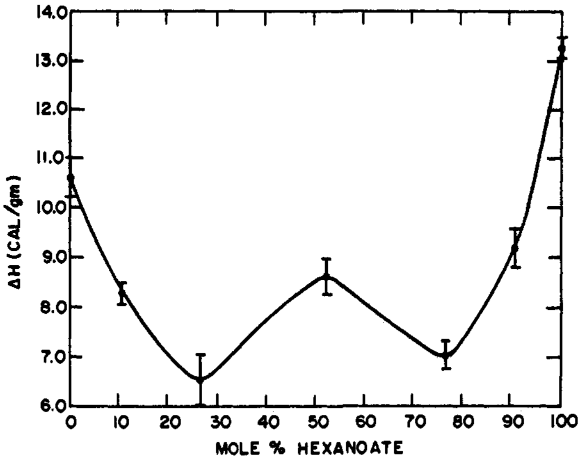

Figure 4. ΔH (fusion) *vs.* composition for cholesteryl nonanoate–cholesteryl hexanoate mixtures.

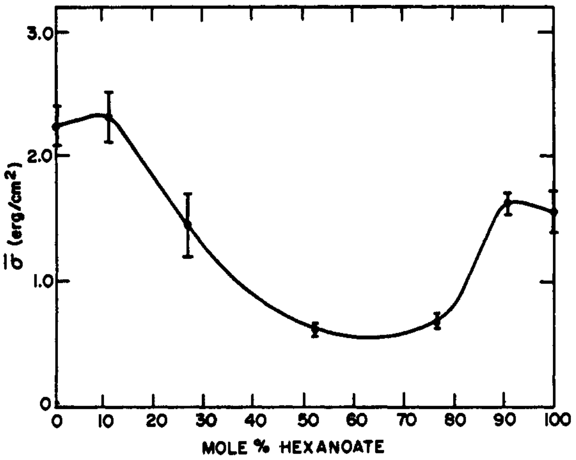

Figure 6. $\bar{\sigma}$ *vs.* composition for cholesteryl nonanoate–cholesteryl hexanoate mixtures.

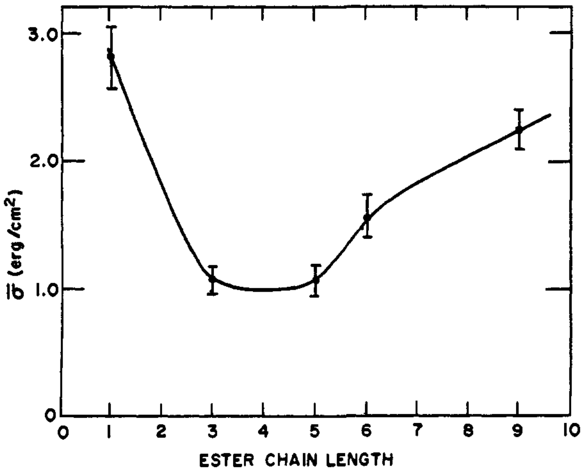

Figure 5. $\bar{\sigma}$ *vs.* ester chain length for the cholesteryl alkanoates.

not obey the Van't Hoff equation[8] and must be considered nonideal solutions. The system exhibits a minimum in the melting point (Figure 3).

The linearity of the liquid crystal to isotropic transition temperature with composition indicates that the mixed liquid crystal phase does behave as a homogeneous solution. This effect has been noted and discussed previously for nematic systems.[9]

Thermodynamic results are listed in Table I. The data for ΔH agree quite well with those of Barrall, Porter, and Johnson.[10] The ΔS for the mixed systems (Table II) does not exhibit any unique variation with composition, but instead reflects the overall effect of ΔH. It is interesting to note that ΔH for the 76.5% hexanoate system is a minimum (Figure 4).

Figures 5 and 6 show graphs of $\bar{\sigma}$ *vs.* cholesteryl ester chain length and percentage cholesteryl hexanoate in cholesteryl nonanoate, respectively. The interfacial free-energy term for the cholesteryl nonanoate–hexanoate mixtures exhibits a minimum and varies by a factor of 4. It would appear that the data could be fit by assuming a third interaction parameter σ_{AB} for the interaction between molecules A and B. We have attempted to analyze these data using the following equation

$$\bar{\sigma} = X_1\bar{\sigma}_{AA} + X_2\bar{\sigma}_{BB} + X_3\bar{\sigma}_{AB} \qquad (8)$$

where $\bar{\sigma}_{AA}$ and $\bar{\sigma}_{BB}$ are the interaction parameters of the pure components and X_1, X_2, and X_3 are statistical percentages represented by various assumed lattice structures in the crystalline state. In all models used $\bar{\sigma}_{AB}$ would have to be negative to allow a fit of the experimental data. A difference in the σ's due to differences in molecular head-to-head or side-to-side interactions was not taken into account in this analysis.

Nucleation data for cholesteryl chloride are also included in Table I. This system displayed a rate curve similar to Figure 1; cholesteryl chloride undergoes thermal decomposition and the data represent only freshly prepared samples.

Because of inability to accurately detect nucleation at temperatures below the rate maximum, E_d has been obtained for only two of the compounds studied: cholesteryl chloride and cholesteryl nonanoate. For the chloride E_d is calculated to be 27.4 ± 2.8 kcal/mol. It is difficult to measure the viscosity of a supercooled liquid crystal, as shearing action facilitates recrystallization. In order to compare our value of E_d with that obtained *via* viscosity measurements for cholesteryl nonanoate, Berg's[11] plot of $\ln \eta$ *vs.* $1/T$ was extrapolated to the supercooled region linearly. The E_d of 9.8 ± 1.0 kcal/mol does not agree with Berg's viscosity activation energy of $\sim$16 kcal/mol. This may be an indication that the microscopic viscosity governing movement across the liquid crystal–crystal interface is different from the bulk viscosity or that our assumption of linearity of $\ln \eta$ *vs.* $1/T$ is not valid.

Discussion

The interfacial energies for the cholesteryl esters and mixtures thereof are an order of magnitude lower than the lowest reported values for other monomeric materials.[3] The values are also much lower than values derived for polymeric systems[2] or inorganics such as selenium.[12] In order for these values to increase one order of magnitude, the value of f(θ) described in the

---

(8) A. R. Ubbelohde, "Melting and Crystal Structure," Clarendon Press, Oxford, 1965, p 235.

(9) J. S. Dave and M. J. S. Dewar, *J. Chem. Soc.*, 4616 (1954).

(10) E. M. Barrall, R. S. Porter, and J. F. Johnson, *J. Phys. Chem.*, 71, 1224 (1967).

(11) D. Berg, *Nat. Acad. Sci.-Nat. Res. Coun., Publ.*, 1356 (1965).

(12) R. G. Crystal, *J. Polym. Sci., Part A-2*, 8, 1755 (1970).

theory section would have to be 10^{-3}. The implication from these values of $\bar{\sigma}$ is that the mesophase is more like the solid phase than the isotropic phase, in accord with the postulate of short-range ordering in the liquid-crystalline state.[13]

The variance of E_d in cholesteryl nonanoate from extrapolated viscosity data may also demonstrate this effect. The lower value of E_d, as compared to a viscosity derived activation energy, may be due to the fact that nucleation and crystal growth are molecular reorientation effects while the viscosity activation energy is due to domain reorientation in the liquid crystal.

Heterogeneous nucleation in the sample has not been taken into account, but all initial nucleation and crystal growth do occur at the liquid crystal–vacuum interface. Our measurement obviously must contain a contribution from crystal growth, since it would be impossible to observe initially stable nuclei. We have made no correction for this effect because Price and coworkers have recently found that for the cholesteryl esters the crystal growth rate over a comparable temperature range is an order of magnitude smaller and temperature independent.[14] Therefore, our rates contain a constant but negligible contribution from crystal growth at all temperatures.

It has been shown by many investigators that there is very little difference thermodynamically between the cholesteric and smectic mesophases,[13,15] *i.e.*, that ΔH and ΔS for interconversion of the two states are small in systems that exhibit both mesophases. Structurally, the cholesteric and smectic phases are quite different; the smectic is a more ordered system represented by overlying layers of parallel molecules, and the cholesteric is represented by domains of molecular planes stacked in a helical configuration. Crystal nucleation from these dissimilar structures would be expected to be different. This difference is manifested in Figure 5. Cholesteryl formate, propionate, pentanoate, and hexanoate do not exist in the smectic phase when supercooled, and $\bar{\sigma}$ decreases with increasing chain length.

It appears that a limiting value of $\bar{\sigma}$ at longer chain lengths might be found for the cholesteric mesophase; however, this can not be verified experimentally because of the existence of a stable smectic phase in the esters with chains longer than C_6. Figure 5 also shows that $\bar{\sigma}$ for cholesteryl nonanoate (a measured smectic-crystal transition) is higher than the $C_3 \rightarrow C_7$ esters (a cholesteric-crystal transition). Cholesteryl chloride, although not a carboxylic ester derivative, fits into this concept. This compound exhibits only the cholesteric mesophase. The shorter length of the chlorine substituent would indicate a higher value of $\bar{\sigma}$ than the formate ester. Experimentally, this is observed.

The interfacial energies for the mixtures of cholesteryl nonanoate and cholesteryl hexanoate are lower than those of the pure components. DSC measurements indicate that even the 10.7% hexanoate sample is entirely cholesteric in the supercooled region studied (see Figure 3). Therefore, these data involve only nucleation from the cholesteric mesophase. The composition dependence of $\bar{\sigma}$ must be due to the randomness of the mixtures at intermediate composition, *i.e.*, the additional entropy effect due to mixing. The addition of the longer ester chain nonanoate to hexanoate appears to create more randomness in the system than the inverse addition. This could be explained by the inability of the hexanoate helical structure to incorporate the longer nonanoate molecule, while in the opposite case, incorporation of the hexanoate sturcture would leave only slight voids in the helical packing of the nonanoate.

As mentioned previously, the low value of $\bar{\sigma}$ for the mixtures may be due to an A–B interaction parameter quite different from the pure component interactions. Additionally the assumption that $\sigma_u = \sigma_e$ may not be valid for these long narrow molecules. As shown by Crystal[12] σ_u and σ_e may vary by an order of magnitude, and the cube root value of the product of σ_e and σ_u^2 may give the impression of a small surface energy, whereas one σ (σ_u or σ_e) may be quite small and the other compensatingly large. The enthalpies of fusion of the mixtures (Table I, Figure 4) all are lower than those of the pure components. Of particular interest is the rapid decrease in ΔH upon addition of a few mole per cent of one component to the other. The lowering of ΔH in the mixtures may result from a disruption of lattice structure and lattice flows.[16] Since the crystal structure of these compounds has not been studied, it is not possible to determine this. As stated previously the systems do show melting point depressions typical of that of normal crystalline systems with added diluents.

In conclusion, we have shown that a nucleation theory derived for isotropic systems can be applied successfully to an intermediate phase, the liquid crystal. We have shown the effect of this structured phase on the magnitude of the interfacial energy and also the effect of cholesteryl ester chain length and mesophase type on the interfacial energy terms.

Acknowledgment. The encouragement and advice of Drs. J. H. Becker, J. M. O'Reilly, and W. H. H. Gunther during this effort is appreciated.

---

[13] G. W. Gray, "Molecular Structure and the Properties of Liquid Crystals," Academic Press, New York, N. Y., 1962, p 66.

[14] Private communication, Professor Fraser Price, University of Massachusetts, Nov 1971.

[15] E. M. Barrall, R. S. Porter, and J. F. Johnson, *J. Phys. Chem.*, **71**, 4, 895 (1967).

[16] J. W. H. Oldham and A. R. Ubbelohde, *Proc. Roy. Soc., Ser. A*, **176**, 50 (1940).